

Photocatalytic performance of Sn-doped and undoped TiO₂ nanostructured thin films under UV and vis-lights

E. Arpaç^a, F. Sayılkan^b, M. Asiltürk^c, P. Tatar^a, Nadir Kiraz^a, H. Sayılkan^{b,*}

^a Akdeniz University, Faculty of Arts and Science, Department of Chemistry, 07100 Antalya, Turkey

^b Inonu University, Faculty of Education, Department of Science, 44280 Malatya, Turkey

^c Inonu University, Faculty of Arts and Science, Department of Chemistry, 44280 Malatya, Turkey

Received 20 April 2006; received in revised form 15 May 2006; accepted 18 June 2006

Available online 21 June 2006

Abstract

Sn-doped and undoped nano-TiO₂ particles have been synthesized by hydrothermal process without solvent at 200 °C in 1 h. Nanostructure-TiO₂ based thin films have been prepared on glass substrate by spin-coating technique. The structure, surface morphology and optical properties of the thin films and the particles have been investigated by element analysis and XRD, SEM, BET and UV–vis–NIR techniques. The photocatalytic performance of the films were tested for degradation of Malachite Green dye in solution under UV and vis-lights. The results showed that (a) hydrothermally synthesized nano-TiO₂ particles are fully anatase crystalline form and are easily dispersed in water, (b) the coated surfaces have nearly super-hydrophilic properties and, (c) the doping of transition metal ion efficiently improved the photocatalytic performance of the TiO₂ thin film.

© 2006 Elsevier B.V. All rights reserved.

Keywords: Nano-TiO₂; Sn-doping; Thin film; Photocatalysis

1. Introduction

In recent years, TiO₂ has proved to be one of the most suitable photocatalysts for widespread environmental application [1–3]. Many organic compounds can be decomposed in aqueous solution in the presence of TiO₂ powders, sols or coatings illuminated with UV or vis-light [4–6]. The excited electrons in the conduction band of the semiconductor, along with corresponding positive holes in the valence band, can be produced by the absorption of light of equal or higher energy relative to the band gap (3.2 eV). The holes react with water molecules or with the hydroxyl ions, thus forming hydroxyl radicals, which are strong oxidants toward organic molecules. The photocatalytic effect of TiO₂ as a photo semiconductor is not new as, for example, shown by Hermann. This effect depends on the lattice defects of TiO₂ and can be quenched considerably by lattice doping [7]. Due to the band gap energy of about 3.2 eV, the light absorption of TiO₂, especially of anatase TiO₂, takes place in

the UV. For this reason, much research is going on at present in order to develop of photocatalytic performance of TiO₂ under visible light because there is much more energy produced by the sunlight in the visible lights regime compared to the UV. The first positive results have been demonstrated by Kisch and co-workers [8–10] with carbon doped photocatalysts [11] and by Taga from Toyota with nitrogen doped catalysts. Sn-doped titania also shows enhanced day-light activity [12]. Due to the large number of possible variations; it is rather difficult to find out the appropriate compositions and concentrations of dopants, especially if lattice doping should be avoided. For these reasons, it is likely that investigations will continue for many years to find suitable and efficient photocatalysts to function under daylight conditions.

In order to synthesize of TiO₂, different processes have been reported, such as sol–gel process [13], hydrolysis of inorganic salts [14], ultrasonic technique [15], microemulsion or reverse micelles and hydrothermal process [16–18]. A multitude of polar or non-polar solvents have been used in these processes. In these processes, high calcination temperature above 450 °C is usually required to form regular crystal structure, except for the hydrothermal process. However, in the meantime, the

* Corresponding author. Fax: +90 422 341 0042.

E-mail address: hsayilkan@inonu.edu.tr (H. Sayılkan).

high temperature treatment can decline the surface area and surface hydroxyl or alkoxide groups on the surface of TiO₂, which provide easy dispersion, are lost. Thus, in this work, the hydrothermal process was selected to synthesize nanosized TiO₂ particles at low temperatures, which seems to be really attractive to further improve the photocatalytic activity of TiO₂. Compared with the other TiO₂ powders, these TiO₂ nanoparticles have several advantages, such as being in fully pure anatase crystalline form, having fine particle size with more uniform distribution and high-dispersion ability either in polar or non-polar solvents, stronger interfacial adsorption and easy coating on different supporting material. Moreover, the hydrothermal process employing aqueous solvents as reaction medium is environmentally friendly since the reactions are carried out in a closed system, and the contents can be recovered and reused after cooling down to room temperature. In this work, photocatalytic activity of Sn-doped and undoped TiO₂ thin films were examined for degradation of Malachite Green (MG) in aqueous solutions under UV and vis-lights and the results were compared.

2. Experimental

2.1. Chemicals and apparatus

The reagents employed were titanium(IV)-*n*-butoxide [Ti(OBuⁿ)₄, 97%, Fluka], as TiO₂ source; hydrochloric acid (Merck, 37%) as catalyst; tin(IV) chloride (Alpha, 98%) as dopant; deionized water as hydrolysis agent; 3-glycidoxypropyltrimethoxysilane (GLYMO, Aldrich, 98%) and tetraethylorthosilicate (TEOS, Aldrich, 98%) as binder reagents; 2-butoxyethanol (2-BuOEtOH, Aldrich, 99%) and ethyl alcohol (EtOH, 96%) as solvents.

Nano-TiO₂ photocatalyst was synthesized by Berghoff model hydrothermal unit interfaced with a temperature (up to 240 °C) and time controller unit. In order to determine the crystal phase, Rigaku Geigerflex D Max/B model X-ray diffractometer (XRD) with Cu K_α radiation ($\lambda = 0.15418$ nm) in the region $2\theta = 10\text{--}70^\circ$ with a step size of 0.04° was used. The average crystallite size of TiO₂ nanoparticles were estimated according to the following Scherrer's equation:

$$d_{hkl} = \frac{k\lambda}{\beta \cos(2\theta)}$$

where d_{hkl} is the average crystallite size (nm), λ the wavelength of the Cu K_α radiation applied ($\lambda = 0.154056$ nm), θ the Bragg's angle of diffraction, β the full-width at half maximum intensity of the peak observed at $2\theta = 25.24$ (converted to radian) and k is a constant usually applied as ~ 0.9 . The BET surface area, average pore diameter and micropore volume of the nanosized-TiO₂ particle was calculated from the N₂ adsorption isotherm using ASAP 2000 model BET analyzer at liquid N₂ temperature. During the BET analysis, sample was degassed at 130 °C for 4 h before N₂ adsorption. Pore size distribution of nano-TiO₂ was computed by DFT plus method. C and H elements in the hydrothermally synthesized TiO₂ particle were analyzed by using element analyzer (LECO 932 Model). Cl was analyzed

by means of potential measurement using Orion 96-17B Model Cl electrode. Surface morphologies of particles and coated surfaces were investigated by scanning electron microscopy (SEM, LEO EVO 40 Model). Contact angles of coatings with water were measured by using a goniometer (RAME HART 100-00 Model). Film thickness of coated surfaces were measured by Perthometer (MAHR-M1 Model).

Dye concentration in the aqueous solution after irradiation was measured by a Varian Carry 5000 model UV-vis-NIR spectrophotometer. Coated glass/dye solution was irradiated with Solar Box 1500 model (Erichsen, Germany) radiation unit with Xe-lamp (690 W m^{-2}) and a controller to change the irradiation time and power input from 390 to 1100 W m^{-2} for different time without cut-off filter and with 400 nm cut-off filter without shaking.

2.2. TiO₂ powder synthesis

Ti(OBuⁿ)₄ was cooled in an ice-bath, then HCl was added within 15 min into cooled solution by drop using a burette. After stirring a few minute at ambient temperature, required amount of tin(IV) chloride was added suddenly. The last solution was stirred until it formed a clear and homogeneous solution at ambient temperature. Then, required amount of water was added within 10 min into the last solution dropwise by burette. HCl/Ti(OBuⁿ)₄, SnCl₄/Ti(OBuⁿ)₄ and H₂O/Ti(OBuⁿ)₄ mol/mol ratios were 0.296, 0.05 and 2.06. The gelation occurred after adding water. The reaction was allowed for 2 h, then the viscose solution was obtained. Sol-solution was then transferred into a 250 ml Teflon crucible, then left in a pre-heated (200 °C) stainless steel autoclave device. The reaction allowed at 200 °C for 1 h. After this time, autoclave was removed from the hydrothermal unit and cooled to room temperature. The as-obtained powders were separated through centrifuging and dried in a vacuum sterilizer. Thus, nanosized TiO₂ crystallite was obtained. The undoped TiO₂ was synthesized described as above without using dopant.

2.3. The preparation of coating solution

Before preparing the coating solution, the TiO₂ sol was prepared. For this purpose, required amount of TiO₂ was dispersed ultrasonically in deionized water without using dispersant. For preparing coating solution, GLYMO was first reacted with TEOS for 10 min, then EtOH was added to this mixture and stirred for 10 min. HCl was allowed to react with GLYMO/TEOS/EtOH for 10 min and finally H₂O was added to GLYMO/TEOS/EtOH and allowed to react for 10 min. This coating solution was prepared at room temperature. Molar composition of each item in the coating solution is given in Table 1.

For preparing the coating solution, TiO₂ sol (2.5 g) was added into the solution (2.5 g) and the mixture was stirred for 30 min. Then, the 2-BuOEtOH (2 g) was added into the prepared mixture and stirred for 40 h. The glass surfaces were coated with this solution using spin-coating technique (1000 rpm, 10 s). The solid ratio of TiO₂ in coating was 52.63%.

Table 1
The composition of the contents of coating solution and experimental conditions

Content	Solution composition	Molar ratio (mol/mol)
TiO ₂	H ₂ O/Ti(OBu ⁿ) ₄	2.06
	HCl/Ti(OBu ⁿ)	0.296
	Sn ⁴⁺ /Ti(OBu ⁿ)	5 (mol/mol, %)
Coating solution	GLYMO/TEOS	1
	H ₂ O/GLYMO	3
	H ₂ O/TEOS	3.3
	HCl/GLYMO	0.0263
	HCl/TEOS	0.0294
	EtOH/GLYMO	5.3
	EtOH/TEOS	5

2.4. Photocatalytic degradation of Malachite Green

The photocatalytic performance of the films was determined by the degradation of Malachite Green (MG) dye solution. The coated glass (5 cm × 5 cm) was immersed into 25 ml aqueous MG solution with a concentration of 20 mg/l in a polystyrene reaction cell which has six separate sample compartments and one cover. The cell was immediately located in the Solar Box ready for UV-irradiation inducing the photochemical reaction to proceed. The coated glass/dye solution was irradiated in the horizontal direction and the distance between the UV lamp and the thin film coated glass/dye solution was kept within 20 cm. The change of MG concentration in accordance with the irradiation time was measured by UV–vis–NIR spectrophotometer under UV and vis-irradiation.

2.5. Catalyst reuse studies

Photocatalytic nano-TiO₂ thin films were repetitively used to degrade MG solution under UV-light. After the first use, so-used catalyst was employed to degrade a fresh MG solution under the same conditions. The process was repeated for three times under UV-light.

3. Results and discussion

3.1. Characterization

The crystalline phase of hydrothermally synthesized TiO₂ samples were analyzed by XRD, and their XRD patterns are shown in Fig. 1. When the XRD patterns were compared with PDF #21–1272 data files it was found that all peaks observed at 25.16°, 37.91°, 48.19°, 55.01° (for undoped TiO₂) and 25.12, 37.88, 48.07 and 54.52 (for Sn-doped TiO₂) 2θ values in the XRD pattern are consistent with anatase (1 0 1), (0 0 4), (2 0 0) and (2 1 1) spacing [19]. The other crystalline forms of TiO₂, rutile and brookite, have not been detected in our characterizations. In addition, no Sn phase, examined according to the sensitivity of XRD method, was found in XRD pattern. Based on the main chemical state of Sn⁴⁺, it can be concluded that Sn ions uniformly dispersed among the anatase crystallite. In the region of 10–80°, the shape of diffractive peaks of the crystal planes of Sn-doped TiO₂ (curve b) is quite similar to that

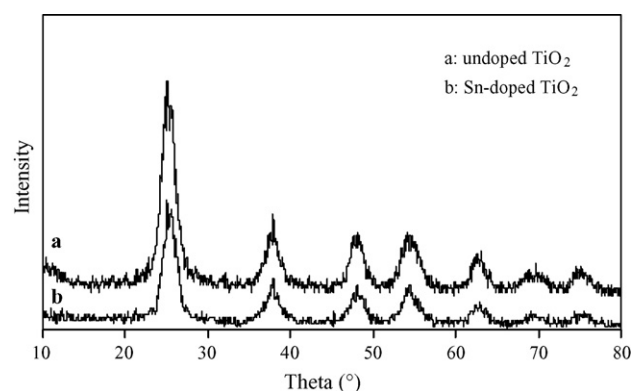


Fig. 1. XRD patterns of nano-TiO₂ particles: (a) undoped TiO₂ and (b) Sn-doped TiO₂.

of undoped TiO₂ (curve a). However, the positions of all the diffraction peaks of the Sn-doped TiO₂ sample was shifted to lower diffraction angles compared with those of TiO₂. According to element analyses, it was determined that the TiO₂ contains 10.49% C, 2.52% H and 2.9% Cl, which means that purity of the TiO₂ is 84.09%.

Some physicochemical characteristics of the synthesized undoped and Sn-doped TiO₂ particles are shown in Table 2.

As can be seen from Table 2, while the BET surface area and adsorption average pore diameter of the undoped TiO₂ are smaller, micropore area, crystallite size and micropore volume are bigger than Sn-doped TiO₂. These properties affect the photocatalytic properties of these photocatalysts. According to the result of DFT plus method, microporosity dominated and distributed very little in the range of 14–20 Å for undoped TiO₂. Whereas, mesoporosity dominated and distributed large area in the range of 12–32 Å for Sn-doped TiO₂. The microporosity (percentage of micropore to total pore volume, V_{mi}/V_{tot}) was obtained almost as 98.6%. Total pore volume was estimated from nitrogen adsorption at a relative pressure of 0.995. The mesoporosity (percentage of mesopore to total pore volume, V_{ms}/V_{tot}) was obtained almost as 1.4%. The mesoporosity and microporosity for Sn-doped TiO₂ were obtained as 79 and 21%, respectively.

UV–vis absorption spectra of Sn-doped and undoped TiO₂ particles are presented in Fig. 2. The doping Sn⁴⁺ results in a sharp increase in the absorption of TiO₂ photocatalyst in visible region, leaving unaffected intrinsic band gap of anatase TiO₂. The greatly red-shift (380–560 nm) can be attributed to the charge–transfer transitions between doped Sn⁴⁺ electrons

Table 2
Some physicochemical characteristics of the synthesized undoped and Sn-doped TiO₂

Property	Undoped TiO ₂	Sn-doped TiO ₂
Crystalline type	Anatase	Anatase
Crystallite size (nm)	9.76	9.24
BET surface area (m ² g ⁻¹)	40.84	97.83
Micropore area (m ² g ⁻¹)	39.3095	19.87
Micropore volume (cm ³ g ⁻¹)	0.022	0.011
Adsorption average pore diameter (Å)	13.12	21.16

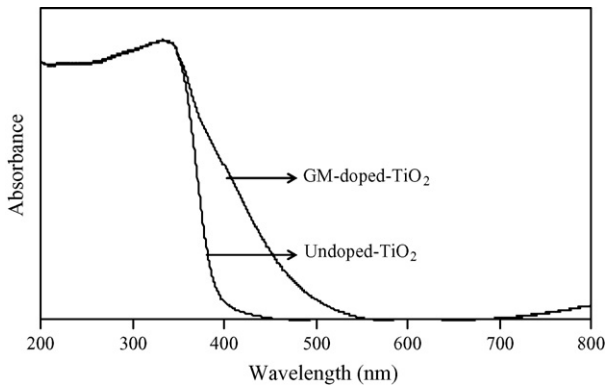


Fig. 2. UV-vis absorption spectra of uncoated and Sn-doped TiO₂ particles.

and the TiO₂ conduction band. The extended absorbance of Sn-doped TiO₂ photocatalyst in the visible region provides a possibility for enhancing the photocatalytic performance of TiO₂.

Typical SEM images of Sn-doped and undoped TiO₂ particles are shown in Fig. 3. Shown in Fig. 3a and b indicating that shape of the particles are quite similar to each other and likely become spherical. However, the size distribution of the powder was not

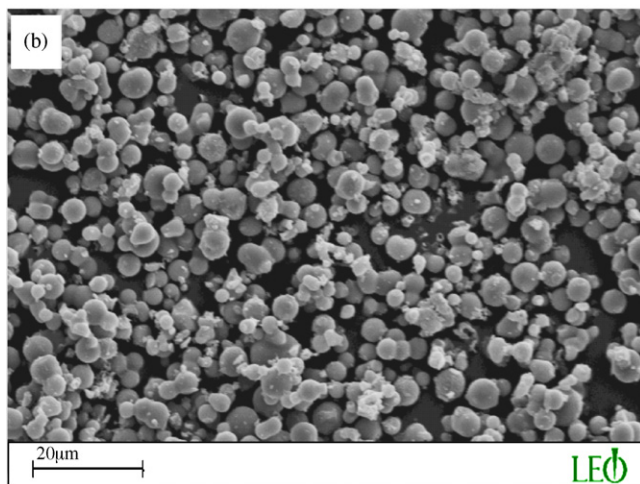
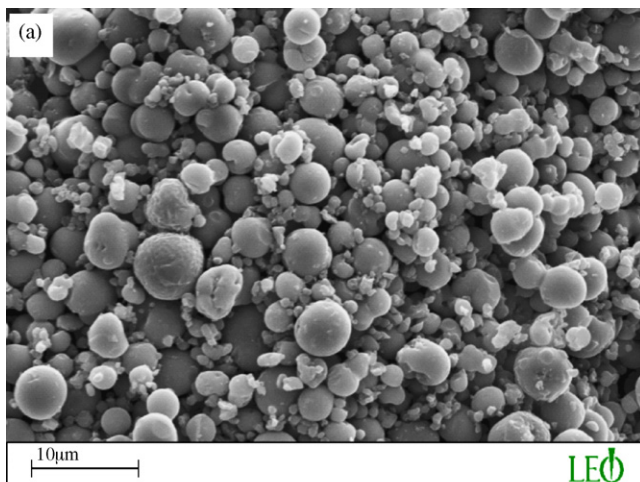


Fig. 3. Typical SEM microphotograph of (a) undoped TiO₂ particle and (b) Sn-doped TiO₂ particle.

Table 3

The results of EDX analysis in three selected points on the undoped and Sn-doped TiO₂ particles

Selected point	Element	wt. %
Undoped TiO ₂		
1	Ti/C/Cl	87.85/6.30/5.85
2	Ti/C/Cl	82.87/10.37/6.76
3	Ti/C/Cl	84.76/11.17/4.07
Sn-doped TiO ₂		
1	Ti/C/Sn/Cl	58.91/24.57/9.51/5.88
2	Ti/C/Sn/Cl	66.34/14.96/11.75/5.96
3	Ti/C/Sn/Cl	66.48/20.20/7.76/4.47

calculated, the size of the particles are varies in the range of 1.12–8.20 μm for Sn-doped TiO₂ and of 2.70–11.72 for undoped TiO₂ as measured using the SEM image. Introduction of Sn⁴⁺ ion decreased the size of the powder and kept a spherical shape.

The results of element analysis (SEM-EDX) carried out locally on the Sn-doped and undoped TiO₂ particles and in three selected points are given in Table 3. According to the analysis points to be selected, the amount of Sn and other elements can be either high or lower. This result indicated that Sn⁴⁺ ions participated on the particle surface was varied little differences.

The glass surface was coated with pre-prepared coating solution using spin-coating technique (1000 rpm, 10 s), and treated at 80 °C for 40 min for curing of the surface. The coated surfaces were irradiated under UV lamp (8 W, UV lamp) for obtaining hydrophilic surface.

Both typical SEM images and three selected points for element analysis (SEM-EDX) of Sn-doped TiO₂ coated glass surfaces are shown in Fig. 4. As can be seen in Fig. 4, the coated surface has very smooth and transparent image. The film thickness was measured as 5–7 μm. The results of element analysis carried out locally on the Sn-doped TiO₂ coated glass surface are given in Table 4. The results in Table 4 showed that the amounts of Si, Sn, Cl and Ti are almost equal to each other in three selected points on the coated surface. In other words, these elements in coating are almost distributed homogeneously on the surface.

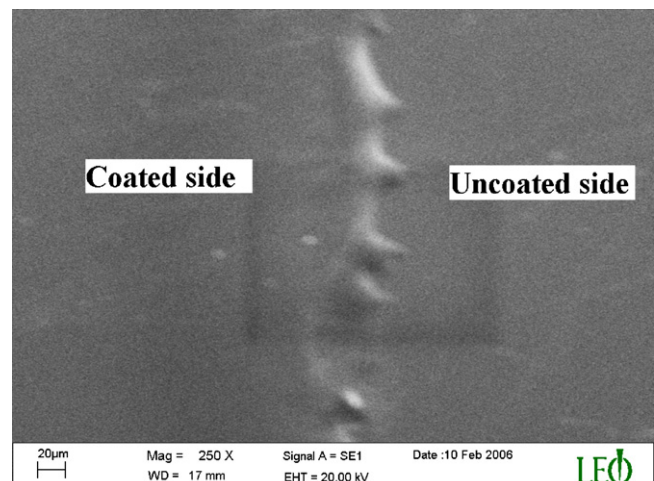


Fig. 4. SEM micrograph of coated glass surface.

Table 4

The results of EDX analysis in three selected points on the Sn-doped TiO₂ coated glass surface

Selected point	Element	wt. %
1	Si/Sn/Cl/Ti	0.73/0.58/0.31/0.14
2	Si/Sn/Cl/Ti	0.81/0.56/0.42/0.13
3	Si/Sn/Cl/Ti	0.67/0.41/0.33/0.12

After the irradiation, the contact angle of the surface with water was found to be 3–5°. The contact angle decreases during the irradiation. For example, while the contact angle was 3–5° on the irradiated surface, it was 60–65° on the unirradiated surface. The decrease in the contact angle can be attributed to the reaction of produced electrons and holes in a different way. According to Fujishima et al. [20] the electrons tend to reduce the Ti(IV) cations to the Ti(III) state and the holes oxidizes the O²⁻ anions. In the process oxygen atoms are rejected, creating oxygen vacancies. Water molecules can then occupy these oxygen vacancies, producing adsorbed OH groups, which tend to make the surface hydrophilic. Therefore, we can conclude that the irradiated surface has almost super-hydrophilic property. This property has an important role for photocatalytic properties. As can be seen from Fig. 5, water drop spreads as a thin film on the irradiated surface.

Sn-doped TiO₂ coated surface exhibited good photocatalytic activity for the degradation of MG under both UV and vis-lights irradiation.

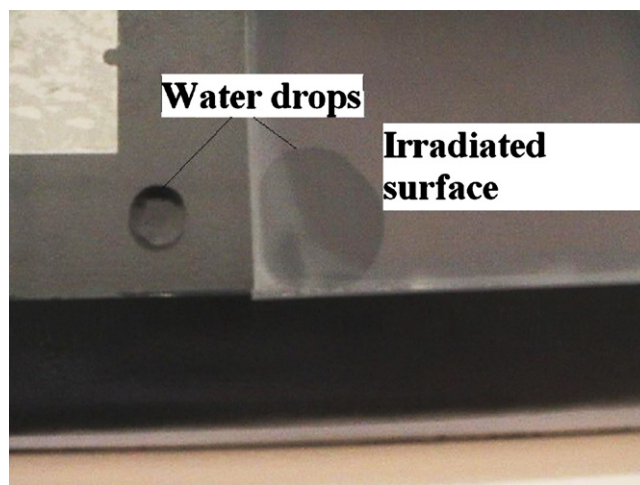


Fig. 5. The water drops images on the irradiated and non-irradiated surfaces.

As shown in Fig. 6, the photocatalytic performance of Sn-doped TiO₂ thin film for the degradation of MG is higher than that of the undoped TiO₂ thin film under UV and vis-lights. According to results of repeated usage experiments performed under UV-light, doping of Sn⁴⁺ ion improves the photocatalytic activity. After the third use, the photocatalytic performance of Sn-doped TiO₂ thin film was almost similar to first and second use, whereas the undoped TiO₂ thin film showed a decreased photocatalytic activity from first to third use. After

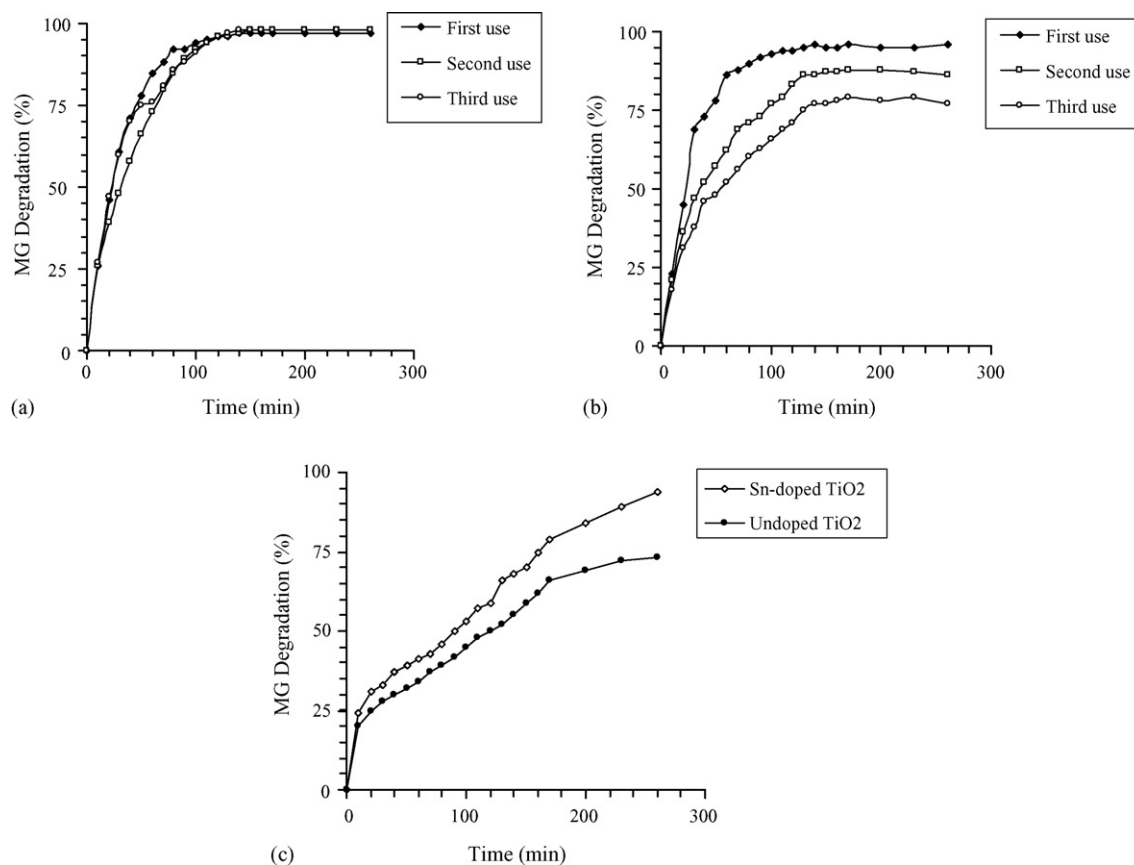


Fig. 6. Photodegradation of MG under UV-light: (a) Sn-doped TiO₂ coated, (b) undoped TiO₂ coated glass surfaces and (c) photodegradation of MG under vis-light.

UV-irradiation for 260 min, the MG (20 mg/l) was degraded as 97, 98 and 98% after first, second and third use with Sn-doped TiO₂ thin film, respectively. On the other hand, the MG was degraded as 96, 86 and 77% with undoped TiO₂ thin film, respectively. In the experiments performed under the vis-light, it was observed that the photocatalytic performances of both thin films increase in the course of time. However, it was observed that doping of Sn⁴⁺ ions improved the photocatalytic performance under visible light irradiation. The MG was degraded as 94% with Sn-doped TiO₂ film whereas it was degraded as 73% with undoped TiO₂ thin film under vis-irradiation.

There are various reasons in the increase photocatalytic performance. These are: (a) the high photocatalytic activity of Sn-doped TiO₂ film may be related to small crystal size, high surface area as well as its mesoporous structure. (b) Dopant Sn⁴⁺ improves electron transfer efficiency from the LUMO band of MG to the conduction band of TiO₂, subsequently increasing the amount of radicals. (c) The high photocatalytic performance, we presume, is ascribed to the Sn ions located in the TiO₂ lattice. The Sn ions can be in the substitutional sites of Ti while a solid-state compound, Ti_{1-x}Sn_xO₂, may be formed [21,22]. The Ti_{1-x}Sn_xO₂ may have a higher photocatalytic performance than undoped TiO₂ and this can result in a high efficiency to degrade MG. At the same time, it is seen that the Sn-doped TiO₂ particle has a stronger UV-light absorption ability than the undoped TiO₂. This also denotes that the Sn-doped TiO₂ particle can effectively be utilized under vis-irradiation for photocatalytic applications. (d) All the nano-TiO₂ particles in coating can be transferred onto the Sn-doped TiO₂ coated surface during the irradiation resulting in a high photocatalytic performance.

4. Conclusion

Nanosized Sn-doped and undoped TiO₂ particles were synthesized by hydrothermal process at low temperature. Very transparent and smooth TiO₂ based thin films were prepared by spin-coating technique. It was obtained that the synthesized nano-TiO₂ particles have an amphiphilic and the coated surfaces have almost super-hydrophilic properties. Doping of the Sn⁴⁺ ion decreases the particle size. The photocatalytic performance of Sn-doped TiO₂ thin film for the photodegradation of MG is

higher than that of the undoped TiO₂ film under UV and vis-lights. It can be suggested that, Sn-doped TiO₂ coated surfaces can be used for preparing self-cleaning and/or antibacterial surfaces.

Acknowledgement

The authors gratefully acknowledge the financial support of T.R. Prime Ministry State Planning Organization (project number: 2005 DPT.120.150).

References

- [1] A. Fujishima, K. Hashimoto, T. Watanabe, TiO₂ Photocatalysis Fundamentals and Applications, BKC Inc., Tokyo, 1999.
- [2] W.C. Tincher, Text. Chem. Color. 21 (1989) 23.
- [3] M.R. Hoffmann, S.T. Martin, W.Y. Choi, D.W. Bahnemann, Chem. Rev. 95 (1995) 69.
- [4] M. Asiltürk, F. Sayılkan, S. Erdemoğlu, M. Akarsu, H. Sayılkan, M. Erdemoğlu, E. Arpaç, J. Hazard. Mater. B129 (2006) 164.
- [5] K. Vinodgopal, P.V. Kamat, Environ. Sci. Technol. 29 (1995) 841.
- [6] J. Liqiang, F. Honggang, W. Baiqi, W. Dejun, X. Baifu, L. Shudan, S. Jiazhong, Appl. Catal. B: Environ. 62 (2006) 282.
- [7] J.M. Herrmann, A. Assabane, A.I. Yahia, H. Tahiri, C. Guillard, Appl. Catal. B: Environ. 24 (2) (2000) 71.
- [8] H. Kisch, W. Lindner, Chemie in unserer Zeit 35 (2001) 250.
- [9] L. Zang, W. Macyk, C. Lange, W.F. Maier, C. Antonius, D. Meissner, H. Kisch, Chem. Eur. J. 6 (2000) 379.
- [10] W. Macyk, H. Kisch, J. Inf. Rec. 25 (2000) 435.
- [11] S. Sakthivel, H. Kisch, Angew. Chem. 115 (40) (2003) 5057.
- [12] J. Yang, D. Li, X. Wang, L. Lu, J. Solid State Chem. 165 (2002) 193.
- [13] G. Colon, M.C. Hidalgo, J.A. Navio, Catal. Today 76 (2002) 91.
- [14] Y. Zhang, G. Xion, N. Yao, W. Yang, X. Fu, Catal. Today 68 (2001) 220.
- [15] X.M. Wu, L. Wang, Z.C. Tan, G.H. Li, S.S. Qu, J. Solid State Chem. 156 (2001) 220.
- [16] E. Vigil, J.A. Ayllon, A.M. Peiro, R.R. Clemente, Langmuir 17 (2001) 891.
- [17] H. Zhang, M. Finnegan, J.F. Banfield, Nano Lett. 1 (2001) 81.
- [18] X. Ju, P. Huang, N. Xu, J. Shi, J. Membr. Sci. 202 (2002) 63.
- [19] I. Kartini, P. Meredith, J.C.D. Da Costa, G.Q. Lu, J. Sol-Gel Sci. Technol. 31 (2004) 185.
- [20] A. Fujishima, T.N. Rao, D.A. Tryk, J. Photochem. Photobiol. C: Photochem. Rev. 1 (2000) 1.
- [21] Y. Cao, W. Yang, W. Zhang, G. Liu, P. Yue, New J. Chem. 28 (2004) 218.
- [22] F. Fresno, C. Guillard, J.M. Coronado, J.M. Chovelon, D. Tudela, J. Soria, J.M. Herrmann, J. Photochem. Photobiol. A: Chem. 173 (2005) 13.